Cobaloxime-based homogeneous and metal-organic framework photocatalytic systems for selective reduction of acetylene to ethylene

Aaron E.B.S. Stone,[1] Xijun Wang,[2] Anna Fortunato,[3] Edoardo Saggioro,[3] Randall Q. Snurr,[2] Francesca Arcudi,[3,*] Joseph T. Hupp,[1,*] and Luka Đorđević[3,*]

[1]*Department of Chemistry, Northwestern University, 2145 Sheridan Rd., Evanston, IL 60208-3113, United States*
[2]*Department of Chemical and Biological Engineering, Northwestern University, 2145 Sheridan Rd., Evanston, IL 60208-3120, United States*
[3]*Department of Chemical Sciences, University of Padova, Via F. Marzolo 1, 35131 Padova, Italy*
*corresponding authors. Email: francesca.arcudi@unipd.it; j-hupp@northwestern.edu; luka.dordevic@unipd.it

ABSTRACT

The semi-hydrogenation of acetylene to ethylene in ethylene-rich gas streams is an industrially important chemical reaction for producing polymer-grade ethylene. Traditional thermocatalytic routes for acetylene reduction to ethylene, despite progress, still require high temperatures and high H_2 consumption, possess low selectivity, and use a noble metal catalyst. Light-powered strategies are starting to emerge, given that they have the potential to use directly the abundant and sustainable solar irradiation. Here we report >99.9% selective, visible-light powered, catalytic conversion of acetylene to ethylene. Our catalyst is a homogeneous molecular cobaloxime that operates in tandem with a photosensitizer at room temperature and bypasses the use of non-environmentally friendly and flammable H_2 gas feed. The reaction proceeds through a cobalt-hydride intermediate with nearly 100% conversion of acetylene under competitive (ethylene co-feed) conditions after only 50 minutes, and with no evolution of H_2 or overhydrogenation to ethane. We further incorporate the cobaloxime as linker in a metal-organic framework; the result is a heterogeneous catalyst for the conversion of acetylene under competitive (ethylene co-feed) conditions that can be recycled up to six times and remains catalytically active for 48 hours, before significant loss of performance is observed.

INTRODUCTION

Ethylene is one of the world's most important commodity chemicals; nearly 200 million tons are produced annually, the most of any organic compound, and ethylene is an intermediate in 50-60% of all plastics.[1,2] The vast majority of ethylene is derived from the steam cracking of petroleum, a process which unavoidably introduces impurities into the crude ethylene stream.[1,3,4] From the standpoint of plastics production, the most pernicious of these contaminants is acetylene, which poisons the Ziegler-Natta catalysts that polymerize ethylene into plastics.[1,3,5,6] Typically, crude ethylene streams contain 0.5-2% acetylene by volume; prior to plastics production, removal of the acetylene impurity is imperative.[1,5,6]

The current industrial standard[5,6] for thermocatalytic acetylene semihydrogenation has weaknesses in that it uses high temperatures and pressures, H_2 co-feed, and precious metal Pd catalysts. This reaction is additionally prone to over-hydrogenation to ethane, a less valuable product that also inhibits polymerization of ethylene, and therefore must be removed using cryogenic sublimation prior to plastics production.[7] The use of Pd and excess H_2 as co-feed limits the ethylene selectivity of the thermocatalytic process to 85% with >90% conversion at 200 °C.[3,5,6,8] Recently, our research groups pursued photocatalytic routes to avoid the drawbacks of the thermochemical routes.[5,6] We sought to improve upon selectivity and conversion by designing photocatalytic systems based on Co-porphyrin catalysts, and succeeded in creating both a homogenous system based on [*meso*-tetra(4-sulfonatophenyl)porphyrinato]-cobalt(III)[9] and a heterogeneous system based on the metal–organic framework (MOF) Co-PCN-222 (with [*meso*-tetra(4-carboxyphenyl) porphyrinato]-cobalt(III) linkers).[10] Notably, both achieved nearly 100% conversion with >99% selectivity for ethylene over ethane under industrially relevant conditions (dilute acetylene in a predominantly ethylene stream). However, long irradiation times (>28 h) are

necessary to achieve photocatalytic conversion of acetylene under a mixed acetylene/ethylene atmosphere (the industrially relevant conditions), with both our homogenous and heterogenous Co-porphyrins systems, which makes it unlikely for the photocatalytic process to be implemented industrially. Therefore, the discovery of novel, more efficient catalysts, and their integration in photocatalytic systems for this industrially relevant transformation remain essential. Combining the high activity, selectivity, and tunability of homogeneous catalysts with the durability and recyclability of heterogeneous catalysts represents a grand achievement in catalysis. Metal–organic frameworks (MOFs) are excellent candidates for achieving this goal through a molecular approach to heterogeneous catalysis. MOFs are a class of porous, crystalline, multi-dimensional nanomaterials composed of inorganic metal ions or clusters (nodes) connected by polytopic organic molecules (linkers).[11,12] Pursuing the use of MOFs in catalysis can offer some additional advantages, such as: (*i*) their chemical stability and high surface areas make them great supports for highly dispersed and well-isolated catalysts;[13-16] (*ii*) the plethora of choices for both the inorganic and organic components of MOFs, allowing for the incorporation of molecular catalysts into the framework as either the node[17-21] or the linker;[22-26] (*iii*) MOFs are also prized for the ease with which they can be post-synthetically modified, which allows catalysts to be installed and distributed throughout the framework after synthesis;[27-34] (*iv*) the crystallinity and long-range order of MOFs make it is possible, in principle, to engineer the same microenvironment for all catalyst species to achieve true single-site catalysis.[35]

In the previously reported photocatalytic reaction conditions for acetylene semi-hydrogenation with cobalt porphyrins, the hydrogenation was proposed to proceed through the acetylene π-complex pathway,[9] which could limit the activity due to protonation of the π-complex being the rate determining step of the catalytic cycle.[36] Alternatively, a metal hydride intermediate could be

used for hydrogen atom transfer (HAT) for the hydrogenation of alkynes.[37] We therefore hypothesized that catalysts capable of performing the HAT reaction *via* a Co^{III}–H intermediate would be good candidates for photocatalytic acetylene hydrogenation. Therefore, to improve upon Co-porphyrin-based systems, and to emphasize the ability of MOFs to stabilize delicate homogeneous catalysts, here we pursue cobaloxime-based systems for the photocatalytic semihydrogenation of acetylene. Cobaloximes are octahedral Co complexes composed of two equatorial dioxime ligands commonly connected by hydrogen bonding (**Figure 1b**). The upward axial ligand is typically a halide, while the downward axial ligand can be either another halide, or a nitrogen base such as pyridine.[38] The relative ease of preparation, together with synthetic flexibility and tunability of the ligand structure, have made cobaloximes a popular choice for development of photocatalytic systems.[39] Cobaloximes are among the most widely studied molecular catalysts for the HER, exhibit excellent activity, and can be paired with myriad organic and inorganic photosensitizers.[38,40,41] Furthermore, it is well-established that cobaloxime-mediated H_2 evolution proceeds through a Co^{III}–H intermediate.[38,41] Cobalt hydride intermediates have been also reported for HAT reaction to organic substrates, which suggests that this method could be extended to acetylene semihydrogenation.[42-45] As they exist in the same phase as the reaction mixture, separation and reuse of molecular cobaloximes from the reaction mixture can be, however, extremely difficult or impossible. Furthermore, molecular cobaloximes are known for their long-term instability due to only hydrogen bonds holding together the equatorial ligand framework.[38,40] To stabilize the cobaloxime motifs, the following strategies can be pursued: (*i*) excess ligand is often added to stabilize the cobaloximes in catalytic studies;[46,47] (*ii*) the internal hydrogen bonding of the oximes can be replaced by difluoroborylate (BF_2) groups;[39,41] and (*iii*) cobaloximes can be stabilized by incorporation into a MOF.[29,40]

Here, we report two novel photocatalytic systems for the semihydrogenation of acetylene to ethylene: one homogeneous system using a molecular cobaloxime and one heterogeneous system based on a metal–organic framework with a cobaloxime linker (**Figure 1**). The catalysts are photosensitized by tris(2,2'-bipyridyl)ruthenium(II) chloride ($[Ru(bpy)_3]^{2+}$). We first developed a photocatalytic system based on the molecular catalyst chloro(pyridine)bis(dimethylglyoximato)cobalt(III) ($[Co(dmgH)_2pyCl]$, dmgH = dimethylglyoxime, py = pyridine), which exhibits excellent catalytic activity for the conversion of acetylene to ethylene with turnover number (TON) = 1,148 and >99.9% selectivity for ethylene vs. ethane after 20 hours of visible-light irradiation. The homogeneous system is also highly competent for ethylene purification (industrially relevant conditions), achieving nearly 100% visible-light powered conversion of acetylene to ethylene in just 50 minutes, with no evidence of over-hydrogenation to ethane, such that the selectivity for ethylene vs. ethane is >99.9%. Detailed mechanistic studies reveal that acetylene semihydrogenation relies on production of a Co^{I} active species that is protonated to form a Co^{III}–H intermediate, as anticipated. The homogeneous system demonstrates limited reusability under the industrial mixture conditions, and the catalytic solution stops working after three re-uses. To increase recyclability and to improve the durability of our system, we translated our homogeneous system into a heterogeneous one by incorporating molecular cobaloxime as linkers in a MOF. Our heterogeneous system displays similarly fast reduction kinetics and excellent selectivity for acetylene semihydrogenation as the homogeneous system. Critically, the MOF-based system retains catalytic activity for more than twice as long as the homogeneous system (48 hours of irradiation) and can be recycled twice as many times before performance deteriorates.

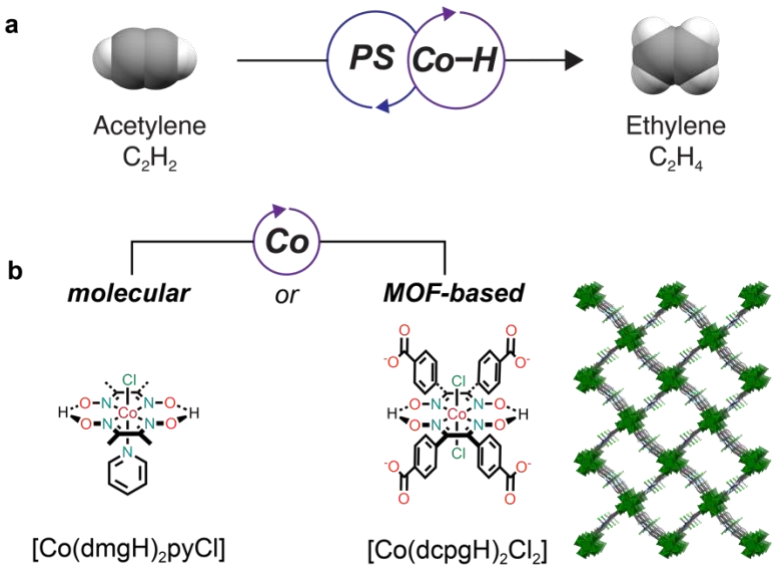

Figure 1. Photocatalytic semi-hydrogenation of acetylene by a cobaloxime-based catalyst through cobalt-catalyzed hydrogen atom transfer reaction. (a) The photocatalytic semihydrogenation of C_2H_2 using cobaloxime-based photocatalytic systems can be achieved using either **(b)** a homogeneous molecular approach or a heterogeneous MOF-based approach.

RESULTS AND DISCUSSION

Chloro(pyridine)cobaloxime(III) Exhibits Excellent Activity and Selectivity for the Photocatalytic Semihydrogenation of Acetylene to Ethylene. *Non-competitive conditions (pure acetylene, no ethylene co-feed)*. Our photocatalytic system consists of four components: [Co(dmgH)$_2$pyCl] as catalyst, $[Ru(bpy)_3]^{2+}$ as photosensitizer (PS), 2,2,2-trifluoroethanol (TFE) as proton source, and 1,3-dimethyl-2-phenyl-2,3-dihydro-1*H*-benzo[*d*]imidazole (BIH) as sacrificial donor (SD). In a typical experiment, we illuminated the catalytic mixture under 1 atm C_2H_2 (≥99.5 vol.%) using a 450 nm light-emitting diode (LED, 140 mW·cm^{-2}); the details of the purging and photocatalytic setups are published elsewhere.[9] Crucially, a typical gas chromatogram and mass spectrum (Figure S1) of the reaction mixture after four hours of irradiation shows conversion of C_2H_2 to C_2H_4 without any appreciable over-hydrogenation to C_2H_6 based on the

limits of detection of our instruments (calibration curves are shown in Figure S2 and Figure S3). We chose BIH and TFE in an attempt to create mild photocatalytic conditions for our cobaloxime catalyst and due to previous reports touting their excellence as SD[29,47-49] and proton source,[50] respectively. A combination of BIH and TFE showed the highest catalytic activity in a screening of various combinations (Figure S4). Based on optimization of the system (Figure S5 and Figure S6), we chose concentrations for each of our reaction components: 2.5 mM $[Ru(bpy)_3]^{2+}$, 1.0 M TFE, 0.1 M BIH, and either 1.0 μM $[Co(dmgH)_2pyCl]$ to maximize turnover number (TON) or 1.0 mM $[Co(dmgH)_2pyCl]$ to maximize conversion of C_2H_2. Illumination for 4 hours of the photocatalytic mixture containing 1.0 mM $[Co(dmgH)_2pyCl]$ produced 63 μmol C_2H_4 (**Figure 2a**) with a quantum yield (QY) of 1.0%, a 10- and 50-fold improvement over our recently investigated Co-porphyrin[9] or Co-PCN-222 system,[10] respectively. In the absence of $[Co(dmgH)_2pyCl]$, $[Ru(bpy)_3]^{2+}$, TFE, BIH, light, or C_2H_2, the C_2H_2 reduction does not occur, which confirms the photocatalytic nature of the reaction (**Figure 2a**). Using 1.0 μM $[Co(dmgH)_2pyCl]$, we obtain TON >1,000 (TON = 1,148) with selectivity for ethylene over ethane >99.9% after 20 hours of illumination (**Figure 2b**). We detected no other gaseous products, except for an extremely small amount of H_2 (2 nmol of H_2 were generated after four hours). As a result, the overall selectivity for C_2H_4 vs. C_2H_6 and H_2 combined is >99.9%.

Depending on the initial concentration of cobaloxime, ethylene production saturates for different reasons. At high cobaloxime concentrations (1.0 mM), catalysis stops due to depletion of BIH, as evidenced by re-addition experiments, in which we first irradiated the system for 20 hours, then selectively re-added various components of the reaction mixture, and irradiated for an additional four hours. These experiments show that it is possible to restart catalysis only upon addition of BIH and no other component of the reaction mixture (Figure S7). At low cobaloxime

concentrations (1.0 µM), however, where the available supply of BIH is not exhausted over the course of the reaction, catalysis most likely ceases due to degradation of the catalyst. Re-addition of [Co(dmgH)$_2$pyCl] restarts catalysis most effectively compared to re-addition of other reaction components (Figure S8). The delicate nature of cobaloxime catalysts has been reported previously,[41,46,47] and our own experiments showing enhanced C_2H_4 production in the presence of excess dimethylglyoxime ligand (Figure S9) are consistent with these previous reports.

The photocatalytic activity of our [Co(dmgH)$_2$pyCl]-based system is not limited to the semi-hydrogenation of acetylene. Illumination for 24 h of our [Ru(bpy)$_3$]$^{2+}$/[Co(dmgH)$_2$pyCl] system and phenylacetylene produces styrene (Figure S10) thus showing that our system is competent to expand the scope of alkyne semi-hydrogenation reactions.

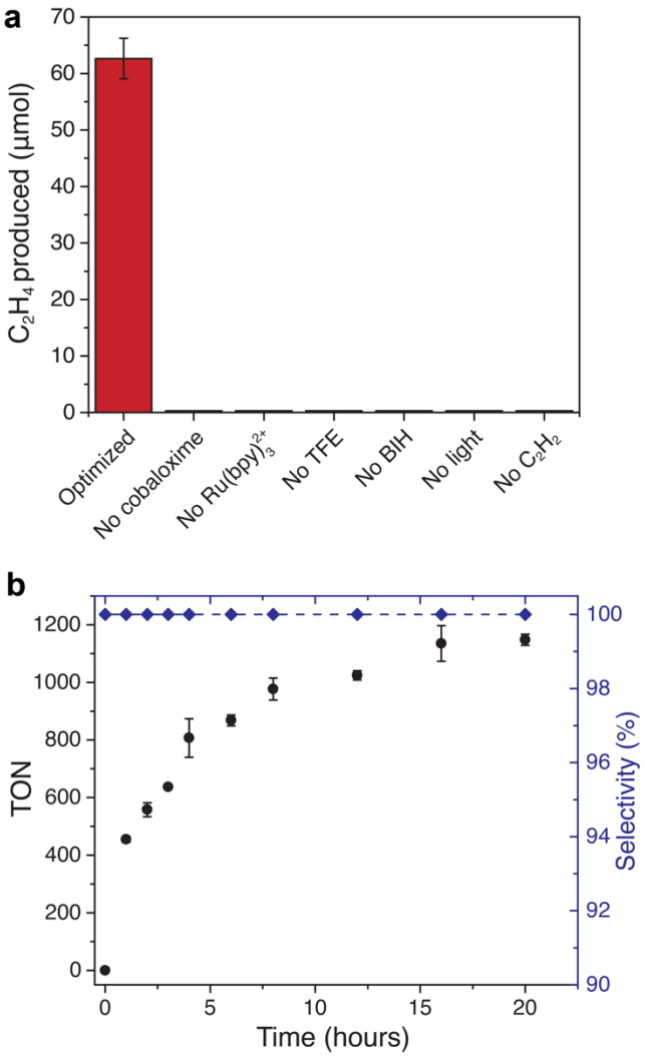

Figure 2. Performance of the homogeneous cobaloxime-based photocatalytic system for the semi-hydrogenation of acetylene to ethylene under noncompetitive conditions (pure acetylene, no ethylene co-feed). (a) Total C_2H_4 production for the optimized reaction mixture containing 2.5 mM $[Ru(bpy)_3]^{2+}$, 1.0 mM $[Co(dmgH)_2pyCl]$, 1.0 M TFE and 0.1 M BIH in acetonitrile irradiated (450 nm, 140 mW·cm^{-2}) for 4 h under C_2H_2 (≥99.5 vol.%), and for reaction mixtures that differ from the optimized conditions as indicated by the axis labels. **(b)** TON (C_2H_4) and C_2H_4 selectivity over C_2H_6 as a function of irradiation time (450 nm) for the $[Ru(bpy)_3]^{2+}$/$[Co(dmgH)_2pyCl]$ system containing 2.5 mM $[Ru(bpy)_3]^{2+}$, 1.0 μM $[Co(dmgH)_2pyCl]$, 1.0 M TFE and 0.1 M BIH in acetonitrile under C_2H_2 (≥99.5 vol.%). Error bars represent the standard deviations for at least three separate experiments.

Competitive conditions (ethylene co-feed). Critically, our $[Co(dmgH)_2pyCl]$-based system selectively reduces C_2H_2 to C_2H_4 even in the presence of excess C_2H_4 (1 vol.% C_2H_2, 30 vol.% C_2H_4, He balance). This C_2H_4/C_2H_2 mixture represents a typical industrial ethylene feed, and a

highly selective catalyst is required to avoid over-hydrogenation to C_2H_6. The performance of our system under industrial mixture conditions is shown in **Figure 3**. Not only does our system reduce the C_2H_2 concentration from 10,000 ppm to undetectable levels without any observed over-hydrogenation to C_2H_6 (**Figure 3ab**, and Figure S11), it does so in less than one hour (50 minutes), which is a 30- and 100-fold improvement over our recently investigated Co-porphyrin (28 hours)[9] or Co-PCN-222 system (87 hours),[10] respectively. Importantly, the calculated production efficiency of our system is ~13 L g^{-1} h^{-1} (liters of ethylene produced over gram of catalyst per hour), which is a factor of ~7 higher than the previously investigated homogeneous batch Co-porphyrin system.[9] We note that our batch-based production efficiency exceeds the industrial demand of >10 L g^{-1} h^{-1},[51] making its industrial implementation promising and could be even further improved in a flow photochemical set-up.[52]

The excellent performance of our system under the industrially relevant conditions allows for its re-use. The same catalytic solution can be purged with fresh industrial gas mixture up to three times before losing its ability to reduce all C_2H_2 in the headspace to C_2H_4 (**Figure 3c**). Additionally, we show that water can be the source of protons for the reaction (Figure S4), which is advantageous from a sustainability standpoint as it avoids the use of an organic, fossil-fuel derived proton source.[53] When the photoreduction was instead performed using D_2O as deuterium source, we observed the formation of C_2D_4 (m/z = 32) from C_2D_2 (m/z = 28), produced by exchange between the feedstock C_2H_2 and D_2O, which we pre-equilibrated before illumination (Figure S12). These two experiments prove that acetylene is the precursor for the observed C_2H_4 and that the protons added to make the C_2H_4 reduction product originate from the water solvent.

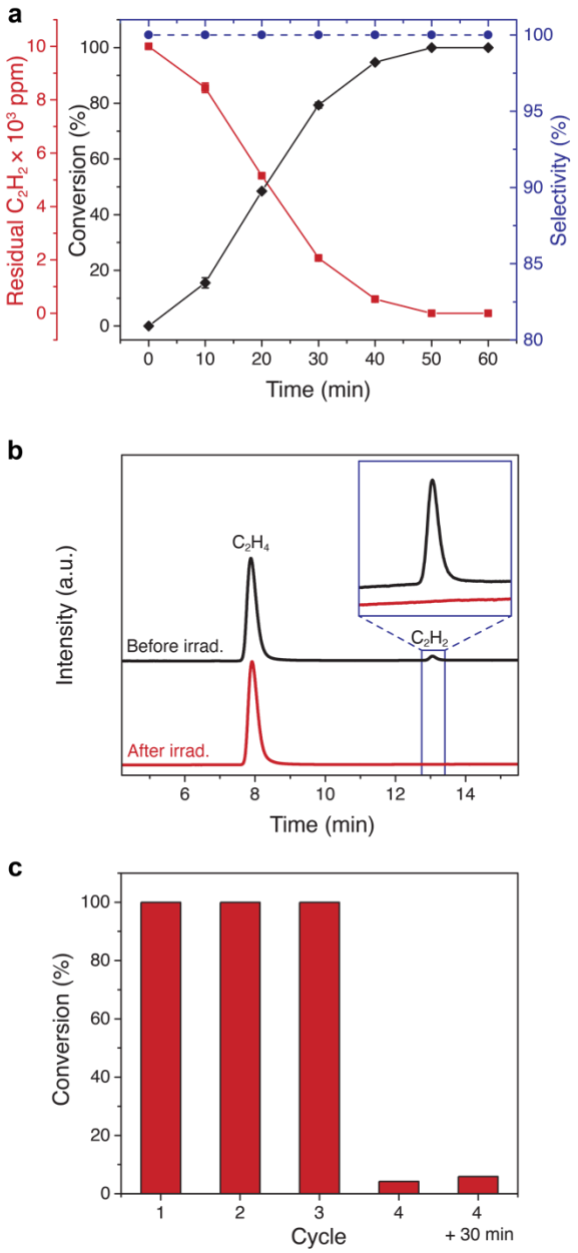

Figure 3. Performance of the homogeneous system under industrially relevant conditions. (a) Plot of C_2H_2 conversion (%), residual C_2H_2 (ppm), and C_2H_4 selectivity vs. C_2H_6 (%) as a function of irradiation time. **(b)** Gas chromatograms (the elution order is C_2H_4, C_2H_6, C_2H_2) detected with flame ion detection before and after irradiation (450 nm) for 50 mins. The inset is a magnified view of the C_2H_2 peak in the chromatogram before and after illumination. **(c)** Reuse of the photocatalytic system under industrial mixture conditions.

Proposed Mechanism. Based on our experimental results and the literature, we propose a mechanism for the photocatalytic semihydrogenation of C_2H_2 to C_2H_4 using our system in **Figure 4a**. Addition of BIH (0.1 M) to a solution of [Co(dmgH)$_2$pyCl] (100 μM) in acetonitrile results in the rapid appearance of a new absorption peak at 423 nm in the UV-Vis spectrum, indicative of a Co^{II} species (**Figure 4b**).[47,54] BIH can therefore chemically reduce [Co(dmgH)$_2$pyCl] from Co^{III} to Co^{II}, and we speculate that this is another reason why re-addition of BIH results in the recovery of catalytic activity at high cobaloxime concentrations. Following light absorption, by $[Ru(bpy)_3]^{2+}$ (PS), the emission of the excited state $[Ru(bpy)_3]^{2+*}$ photosensitizer (PS*) is quenched by hole transfer to BIH to form $[Ru(bpy)_2(bpy^{\bullet-})]^{+}$ ($PS^{\bullet-}$), followed by electron transfer from $PS^{\bullet-}$ (reduction potential of −1.33 V vs. SCE in acetonitrile)[55] to the Co^{II} (Co^{II}/Co^{I} reduction potential of −1.13 V vs. SCE in acetonitrile)[41,54] to form the low valent Co^{I} species. We observed that the unimolecular quenching rate constant for BIH exceeds that of [Co(dmgH)$_2$pyCl] by a factor of nearly 100 according to Stern-Volmer analysis (**Figure 4c**). As a result, we unambiguously conclude that $[Ru(bpy)_3]^{2+}$ photoluminescence is reductively quenched in the presence of BIH, due to the potency of BIH as an electron donor.

We found direct spectroscopic evidence for a reactive Co^{I} intermediate in UV-Vis studies of our system. Irradiation of a solution containing [Co(dmgH)$_2$pyCl], $[Ru(bpy)_3]^{2+}$, and BIH results in the rapid formation of two new absorption peaks at 530 and 656 nm in the UV-Vis spectrum (**Figure 4d**). These peaks have previously been assigned to the formation of a Co^{I} intermediate.[47,56] Upon either 1) purging this solution with C_2H_2 or 2) adding 1.0 M TFE, the Co^{I} signature peaks disappear, and the original absorption profile of Co^{III} complex is recovered (Figure 4d). Taken together, these results confirm the formation of a Co^{I} intermediate that can react with a proton source to form a Co^{III}–H or C_2H_2 directly to form a Co^{III}-C_2H_2 adduct, suggesting that there are

two possible mechanisms for acetylene reduction. We also observe a substantial decrease in evolved H_2 from our system under 99.5% C_2H_2 atmosphere compared to under Ar atmosphere (**Figure 4e**), suggesting again that H_2 evolution and C_2H_2 reduction proceed *via* the same intermediate, and that C_2H_2 reduction outcompetes H_2 evolution under our experimental conditions. It is well-established that photocatalytic H_2 evolution with cobaloxime catalysts proceeds *via* a Co^{III}–H intermediate,[38,41,46,47] and consequently we hypothesized that C_2H_2 semihydrogenation also proceeds through a Co^{III}–H intermediate. We observe no C_2H_2 reduction in the presence of the radical trap TEMPO (**Figure 4f**), which also implies the existence of a radical intermediate. The formation of the TEMPO-acetylene adduct was confirmed by LCMS analysis of the reaction mixture (**Figure 4g**). We conclude that C_2H_2 associates with the cobaloxime catalyst through hydrogen atom transfer (HAT) as opposed to migratory insertion, as HAT generates a radical intermediate and migratory insertion does not.[57] While a Co^{III}-C_2H_2 adduct may form, we believe that this is at most a minor pathway. Since no C_2H_4 production is observed in the absence of a proton source, we suggest that protonation of the Co^{I} intermediate to generate a Co^{III}–H is due to TFE as opposed to BIH in the full reaction mixture. While BIH can act as a proton donor once C_2H_2 is added, BIH is not a potent enough proton donor to react with Co^{I} directly, which explains the persistence of Co^{I} in Figure 4d prior to the addition of C_2H_2. In contrast, TFE can react with Co^{I} directly to form Co^{III}–H, as shown in Figure 4d.

Electrochemical results of [Co(dmgH)$_2$pyCl] provide further evidence of the reactivity of the Co^{I} intermediate. The cyclic voltammogram (CV) of [Co(dmgH)$_2$pyCl] recorded in an Ar-saturated solution shows a (pseudo)reversible redox peak at −1.58 V (vs Fc/Fc^{+}) corresponding to the $Co^{II/I}$ couple (Figure S13). The potential of the $Co^{II/I}$ reversible redox wave is shifted anodically by 45 mV with TFE added to the Ar-saturated solution of [Co(dmgH)$_2$pyCl], which can be

attributed to the equilibrium between Co^{I} and Co^{III}–H (Figure S13). When the CV of $[Co(dmgH)_2pyCl]$ is recorded under C_2H_2, the addition of TFE to the electrolyte causes the rise in catalytic current coupled with the Co^{II}/Co^{I} reduction event (**Figure 4h**). Taken together, these results offer additional support to the formation of a Co^{III}–H intermediate in the photocatalytic mechanism, and that TFE is the primary source of protons in the reaction.

According to our analysis, ethylene production is initiated by Co^{III}–H, followed by HAT to acetylene to form a vinyl radical that may undergo a radical pair collapse to form a vinyl-cobalt species. Aided by density functional theory (DFT) calculations we note that the vinyl-cobalt intermediate contains a weak Co–C bond (46.1 kcal mol^{-1}), which resembles diradicals.[37,58] The strength of the Co^{III}–H bond (49.9 kcal mol^{-1}) matches the C–H bond of the vinyl radical (48.0 kcal mol^{-1}), further supporting the thermodynamic feasibility of the HAT process. Calculations also support the thermodynamically favorable HAT process (ΔG = −17.9 kcal mol^{-1}, **Figure 4i**) that leads from Co–H to Co-vinyl formation. Consistently, the relatively weak Co−H (49.9 kcal mol^{-1}) and Co−C (46.1 kcal mol^{-1}) bond strengths in the Co–cobaloxime complexes indicate that a radical type of HAT pathway is probable.

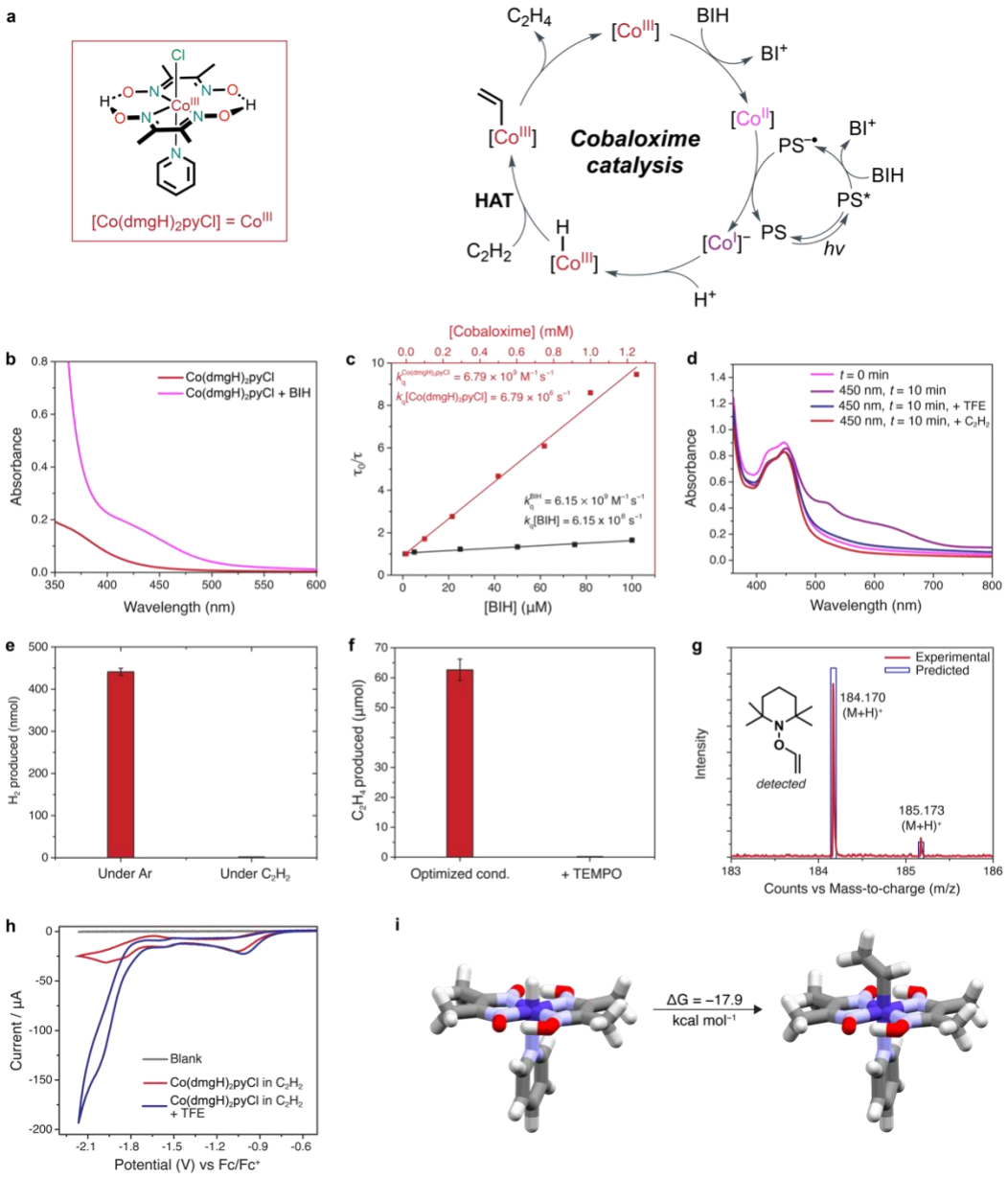

Figure 4. Proposed mechanism of C_2H_2 semi-hydrogenation. (a) Proposed catalytic mechanism for the photocatalytic reduction of C_2H_2 to C_2H_4 using [Co(dmgH)$_2$pyCl]. **(b)** UV-Vis spectra of the 100 μM [Co(dmgH)$_2$pyCl] without (red) and with (magenta) 0.1 M BIH. **(c)** Stern-Volmer plots for the quenching of $[Ru(bpy)_3]^{2+}$ emission lifetime by [Co(dmgH)$_2$pyCl] (red) or BIH (black). **(d)** H_2 evolution by the [Co(dmgH)$_2$pyCl]-based system under Ar vs. C_2H_2. **(e)** UV-Vis spectra of the system containing 100 μM [Co(dmgH)$_2$pyCl], 50 μM $[Ru(bpy)_3]^{2+}$ and 0.1 M BIH under various conditions. **(f)** Comparison of C_2H_4 production by the [Co(dmgH)$_2$pyCl]-based system under optimized conditions and in the presence of 200 molar equiv. TEMPO with respect to [Co(dmgH)$_2$pyCl]. **(g)** Detection of the TEMPO-acetylene adduct using LCMS. **(h)** Cyclic voltammograms of [Co(dmgH)$_2$pyCl] without (red) and with (blue) TFE in acetonitrile (TBA•PF_6 as supporting electrolyte) and saturated with C_2H_2. **(i)** Density functional theory optimized structures for cobaloxime-hydride and cobaloxime-vinyl complexes involved in the HAT reaction. Error bars represent the standard deviations for at least three separate experiments.

Overall, our proposed mechanism is as follows: chemical reduction by BIH (or photoreduction by $[Ru(bpy)_2(bpy^{\bullet-})]^+$) reduces the Co center in $[Co(dmgH)_2pyCl]$ from Co^{III} to Co^{II}. A subsequent photoreduction by $[Ru(bpy)_2(bpy^{\bullet-})]^+$ yields the Co^I intermediate, which reacts with a proton (from TFE proton source) to form a Co^{III}–H species. Then, C_2H_2 inserts into the Co^{III}–H bond *via* HAT. Addition of another proton and dissociation of C_2H_4 regenerates Co^{III} and completes the catalytic cycle.

Integration of a Cobaloxime into a Metal–Organic Framework. In an effort to increase the robustness of our $[Co(dmgH)_2pyCl]$-based photocatalytic system and to endow recyclability, we sought to create a heterogeneous version of our photocatalytic system by using a cobaloxime as the linker in a MOF. Following previously employed strategies,[40,59] we synthesized a polytopic cobaloxime linker ($[Co(dcpgH)_2Cl_2]$, dcpgH = 4,4′-(1,2-bis(hydroxyimino)ethane-1,2-diyl)dibenzoic acid) with four carboxylate anchors for binding to hexazirconium(IV) nodes, which yielded ZrCo-MOF. The PXRD pattern of the obtained material shows intense peaks in the low angle range, characteristic of porous materials (**Figure 5a**). The two major reflections at $\sim 4.5^\circ$ and $\sim 9^\circ$ indicated a long-range order along the *c*-axis, and this is consistent with the previous partially collapsed framework structure obtained after DMF solvent removal.[40,59] The partially collapsed structure is also supported by SEM imaging, which shows spherical particles (Figure S18). The XPS spectrum of ZrCo-MOF is nearly identical to that of $[Co(dmgH)_2pyCl]$, showing that the Co in the MOF remains Co^{3+} following MOF synthesis (**Figure 5b**). The UV-Vis spectrum of ZrCo-MOF indicates successful incorporation of $[Co(dcpgH)_2Cl_2]$ into the framework, as we observe absorption bands similar to those of the molecular cobaloxime (**Figure 5c**). Elemental

analysis using ICP-OES reveals that there are 2.4 Co/Zr_6 node, further supporting successful incorporation of the cobaloxime linker. Taken together, we conclude from these results that we successfully synthesized a Zr-based MOF with cobaloxime linkers, thus creating a solid-state version of our homogeneous molecular photocatalyst.

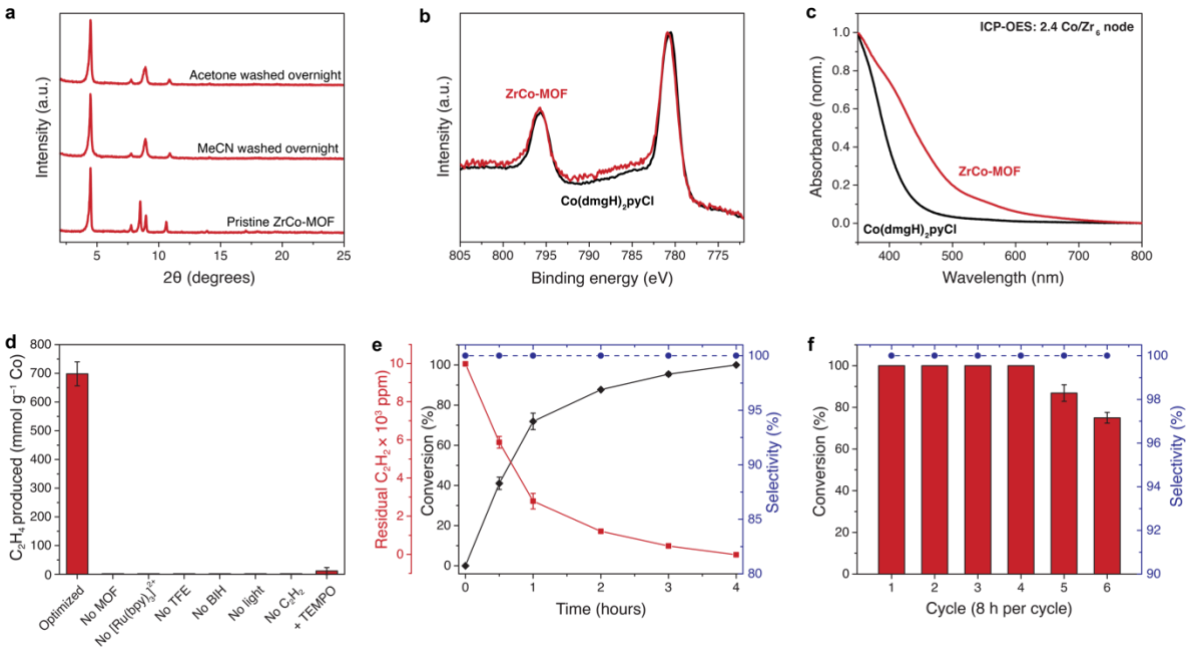

Figure 5. Characterization of ZrCo-MOF and its photocatalytic performance. (a) PXRD patterns of pristine ZrCo-MOF, and ZrCo-MOF soaked in acetonitrile or acetone. **(b)** XPS spectra of [$Co(dmgH)_2pyCl$] (black) and ZrCo-MOF (red). **(c)** UV-Vis spectrum of [$Co(dmgH)_2pyCl$] (black) and DR-UV-Vis spectrum of ZrCo-MOF (red). (**d**) Total C_2H_4 production for the optimized reaction mixture containing 2.5 mM $[Ru(bpy)_3]^{2+}$, 2.28 mg ZrCo-MOF (1 mM cobaloxime concentration), 1.0 M TFE and 0.1 M BIH in acetonitrile irradiated (450 nm, 140 mW·cm^{-2}) for 4 h under C_2H_2 (≥99.5 vol.%), and for reaction mixtures that differ from the optimized conditions as indicated by the axis labels. **(e)** Plot of C_2H_2 conversion (%), residual C_2H_2 (ppm), and C_2H_4 selectivity vs. C_2H_6 (%) as a function of irradiation time. **(f)** Recyclability of the photocatalytic system under industrial mixture conditions. Error bars represent the standard deviations for at least three separate experiments.

Performance of the MOF-Based Heterogeneous System. The heterogeneous version of our homogeneous photocatalytic system using ZrCo-MOF as the catalyst achieves comparable activity

and selectivity to the homogeneous system, while also displaying increased longevity, robustness, and recyclability. Illumination for 4 hours of the ZrCo-MOF-based system produced 698 mmol C_2H_4 per gram of Co (**Figure 5d**), which is a factor of five higher than that our previous Co-PCN-222-based MOF system.[10] No C_2H_4 was produced in the absence of catalyst, sensitizer, sacrificial donor, proton donor, light or C_2H_2 feedstock (**Figure 5d**). We observed that the ZrCo-MOF-based system only produced 11 mmol C_2H_4 per gram of Co when we run the reaction in the presence of TEMPO (**Figure 5d**), which suggests the presence of a radical intermediate similar to the homogenous [Co(dmgH)$_2$pyCl]-based system.

The kinetics of the ZrCo-MOF-based heterogeneous system under the industrially relevant conditions are shown in **Figure 5e**. The ZrCo-MOF-based system selectively photoreduces the C_2H_2 concentration to sub-ppm levels after four hours of illumination. We prepared the samples of the MOF system to have the same number of moles of cobaloxime as the homogeneous samples; we speculate that the MOF-based system takes longer to achieve complete C_2H_2 conversion due to diffusional limitations and reduced access to the catalytic sites on the interior of the framework. We note, however, that this is still a drastic improvement compared to the 87 hours required for our previous Co-PCN-222-based MOF system[10] to fully remove C_2H_2 from the industrial mixture, and compared to the 68 hours required by recently reported metal–organic framework nanosheets[60] to reduce acetylene concentration below 5 ppm. Crucially, like the homogeneous system, no over-hydrogenation to C_2H_6 is observed, such that the selectivity for C_2H_4 remains >99.9% (Figure 5e).

The homogeneous system persists for three cycles and four hours in total before losing its ability to fully reduce C_2H_2 in the industrial mixture. In contrast, the ZrCo-MOF-based heterogeneous system can be recycled up to six times, and remains catalytically active for 48 hours before significant loss of performance (**Figure 5f**). PXRD patterns collected periodically over the course

of the reaction demonstrate retention of crystallinity, even after 48 hours of irradiation (Figure S17). Similarly, SEM images taken at various time points indicate retention of particle morphology (Figure S18). Furthermore, elemental analysis of the MOF powder after photocatalysis indicates that only a small amount of Co leaching occurs over the course of the reaction: according to ICP-OES, there are 2.3 Co/Zr_6 node after both 4 and 24 hours of continuous photocatalysis, and 2.0 Co/Zr_6 node after 48 hours of photocatalysis, inclusive of repeated centrifugation and washing of the recycling experiment. Compared with the 2.4 Co/Zr_6 node present in pristine ZrCo-MOF, this represents a small loss of Co, and we therefore conclude that the loss of catalytic activity is not due to Co leaching, which is further corroborated by ICP-OES of the supernatant from the catalytic mixture after 24 hours of catalysis indicating that only 10.4 ± 1.6% of cobalt in the original ZrCo-MOF leaches in that time. We therefore speculate that the reason catalysis ceases is similar to the homogeneous molecular system, as opposed to degradation of the MOF.

CONCLUSIONS

In conclusion, we have developed a novel photocatalytic system based on a molecular cobaloxime catalyst for the semihydrogenation of acetylene to ethylene, under visible light irradiation and at room temperature. In homogenous conditions, at dilute catalyst conditions, the system achieves TON >1,000 after 20 hours of illumination with >99.9% selectivity for ethylene vs. ethane. At concentrated catalyst conditions, the system produces 63 μmol C_2H_4 after four hours of irradiation with a quantum yield (QY) of 1.0%, a 10- and 50-fold improvement over our recently investigated Co-porphyrin or Co-PCN-222 system, respectively.[9,10] Furthermore, the cobaloxime-based system completely reduces the acetylene in a dilute acetylene co-feed with ethylene (the

industrially relevant conditions) without any detectable over-hydrogenation to ethane in just 50 minutes, which represents a more than 30- and 100-fold improvement over our recently investigated Co-porphyrin systems, respectively.[9,10] The production efficiency of our system is ~13 L g^{-1} h^{-1}, which exceeds the industrial demand of >10 L g^{-1} h^{-1}. Investigation of the mechanism reveals the importance of a Co^{I} species that becomes protonated to form Co^{III}–H (i.e. Co^{III}–hydride), to which acetylene inserts *via* HAT. To improve the durability and recyclability of the homogeneous system, we engineered a heterogeneous version by using a molecular cobaloxime as the linker in a MOF. With the industrial mixture composition, our MOF-based system exhibited the same excellent selectivity (albeit with slightly lower activity) as the homogeneous system, reducing the acetylene concentration to sub-ppm levels with no observed over-hydrogenation within four hours, which represents a ~20-fold improvement over the two recently reported MOF-based systems.[9,10] Importantly, our MOF-based system displayed increased longevity and recyclability over the homogeneous system, maintaining catalytic activity for 48 hours over six cycles.

Besides the higher activity of both the homogeneous and heterogeneous systems compared to their Co-porphyrin counterparts, ZrCo-MOF exhibits greater stability under the reaction conditions than Co-PCN-222,[10] most likely due to the elimination of triethanolamine as sacrificial donor. A further improvement to the system described here would be the elimination of organic solvent: while we demonstrate here that the [$Co(dmgH)_2pyCl$]-based system can use water as the source of protons, ZrCo-MOF lacks the requisite stability in water to make such a heterogeneous system feasible. Alternative MOF-based systems based on water-stable MOFs should be investigated. Additionally, while cobaloximes are cheaper and easier to prepare than porphyrins, the preparation of [$Co(dcpgH)_2Cl_2$] linker is a multi-step synthesis and therefore simpler cobalt-

containing MOFs, such as MOFs that utilize Co as the node[61] or incorporation of catalysts through solvent-assisted ligand incorporation,[62] is an intriguing direction with more potential for industrial scale up.

Overall, the photocatalytic strategies described here avoid the use of noble metal catalysts, high temperatures and pressures, and H_2 gas feed, all while achieving significantly higher selectivity than the current industry standard. This work is a significant step forward for the photocatalytic production of polymer-grade ethylene. We hope that this work stimulates further exploration into photocatalytic and MOF-based systems for the semi-hydrogenation of acetylene to ethylene and their integration into flow cells for crude ethylene purification.

ACKNOWLEDGMENTS

This work was co-funded by the European Union (ERC, PhotoDark, 101077698). Views and opinions expressed are however those of the authors only and do not necessarily reflect those of the European Union or the European Research Council. Neither the European Union nor the granting authority can be held responsible for them. F.A. gratefully acknowledges support from the Italian Ministry of University and Research (Rita Levi Montalcini Program) and the Fondazione Cariparo (Starting Package Program). J.T.H. gratefully acknowledges support from the U.S. Dept. of Energy, Office of Science, Basic Energy Sciences, Solar Photochemistry Program (grant numbers DE-FG02-87ER-13808). R.Q.S. acknowledges support from U.S. Department of Energy, Office of Science, Basic Energy Sciences, Separation Science Program (grant number DE-FG02-08ER15967).We are grateful to Prof. Sascha Ott (Uppsala University) for sharing the structural model of the cobaloxime-MOF.

REFERENCES

1. S. Zhou, L. Shang, Y. Zhao, R. Shi, G. I. N. Waterhouse, Y.-C. Huang, L. Zheng and T. Zhang, *Adv. Mater.*, 2019, **31**, 1900509.
2. R. Geyer, J. R. Jambeck and K. L. Law, *Sci. Adv.*, 2017, **3**, e1700782.
3. Y. Guo, Y. Huang, B. Zeng, B. Han, M. Akri, M. Shi, Y. Zhao, Q. Li, Y. Su, L. Li, Q. Jiang, Y.-T. Cui, L. Li, R. Li, B. Qiao and T. Zhang, *Nat. Commun.*, 2022, **13**, 2648.
4. D. S. Sholl and R. P. Lively, *Nature*, 2016, **532**, 435-437.
5. A. Borodziński and G. C. Bond, *Catal. Rev.*, 2006, **48**, 91-144.
6. F. Studt, F. Abild-Pedersen, T. Bligaard, R. Z. Sørensen, C. H. Christensen and J. K. Nørskov, *Science*, 2008, **320**, 1320-1322.
7. T. Ren, M. Patel and K. Blok, *Energy*, 2006, **31**, 425-451.
8. M. Armbrüster, K. Kovnir, M. Friedrich, D. Teschner, G. Wowsnick, M. Hahne, P. Gille, L. Szentmiklósi, M. Feuerbacher, M. Heggen, F. Girgsdies, D. Rosenthal, R. Schlögl and Y. Grin, *Nat. Mater.*, 2012, **11**, 690-693.
9. F. Arcudi, L. Đorđević, N. Schweitzer, S. I. Stupp and E. A. Weiss, *Nat. Chem.*, 2022, **14**, 1007-1012.
10. A. E. B. S. Stone, L. Đorđević, S. I. Stupp, E. A. Weiss, F. Arcudi and J. T. Hupp, *ACS Energy Lett.*, 2023, **8**, 4684-4693.
11. A. J. Howarth, A. W. Peters, N. A. Vermeulen, T. C. Wang, J. T. Hupp and O. K. Farha, *Chem. Mater.*, 2017, **29**, 26-39.
12. A. J. Howarth, Y. Y. Liu, P. Li, Z. Y. Li, T. C. Wang, J. Hupp and O. K. Farha, *Nat. Rev. Mater.*, 2016, **1**.
13. A. Corma, H. García and F. X. Llabrés i Xamena, *Chem. Rev.*, 2010, **110**, 4606-4655.
14. J. Lee, O. K. Farha, J. Roberts, K. A. Scheidt, S. T. Nguyen and J. T. Hupp, *Chem. Soc. Rev.*, 2009, **38**, 1450-1459.
15. Q. Wang and D. Astruc, *Chem. Rev.*, 2020, **120**, 1438-1511.
16. J. D. Xiao and H. L. Jiang, *Acc. Chem. Res.*, 2019, **52**, 356-366.
17. K. G. M. Laurier, F. Vermoortele, R. Ameloot, D. E. De Vos, J. Hofkens and M. B. J. Roeffaers, *J. Am. Chem. Soc.*, 2013, **135**, 14488-14491.
18. D. Wang, R. Huang, W. Liu, D. Sun and Z. Li, *ACS Cat.*, 2014, **4**, 4254-4260.
19. D. Wang, M. Wang and Z. Li, *ACS Cat.*, 2015, **5**, 6852-6857.
20. J. Long, S. Wang, Z. Ding, S. Wang, Y. Zhou, L. Huang and X. Wang, *Chem. Commun.*, 2012, **48**, 11656-11658.
21. P. Li, R. C. Klet, S. Y. Moon, T. C. Wang, P. Deria, A. W. Peters, B. M. Klahr, H. J. Park, S. S. Al-Juaid, J. T. Hupp and O. K. Farha, *Chem. Commun.*, 2015, **51**, 10925-10928.
22. M.-H. Xie, X.-L. Yang, C. Zou and C.-D. Wu, *Inorg. Chem.*, 2011, **50**, 5318-5320.
23. J. A. Johnson, X. Zhang, T. C. Reeson, Y.-S. Chen and J. Zhang, *J. Am. Chem. Soc.*, 2014, **136**, 15881-15884.
24. H.-Q. Xu, J. Hu, D. Wang, Z. Li, Q. Zhang, Y. Luo, S.-H. Yu and H.-L. Jiang, *J. Am. Chem. Soc.*, 2015, **137**, 13440-13443.
25. Y. Chen, T. Hoang and S. Ma, *Inorg. Chem.*, 2012, **51**, 12600-12602.
26. D. W. Feng, Z. Y. Gu, J. R. Li, H. L. Jiang, Z. W. Wei and H. C. Zhou, *Angew. Chem. Int. Ed.*, 2012, **51**, 10307-10310.
27. A. W. Peters, Z. Li, O. K. Farha and J. T. Hupp, *ACS Appl. Mater. Interfaces*, 2016, **8**, 20675-20681.

28. C. Gomes Silva, I. Luz, F. X. Llabrés i Xamena, A. Corma and H. García, *Chem. Eur. J.*, 2010, **16**, 11133-11138.
29. P. M. Stanley, A. Y. Su, V. Ramm, P. Fink, C. Kimna, O. Lieleg, M. Elsner, J. A. Lercher, B. Rieger, J. Warnan and R. A. Fischer, *Adv. Mater.*, 2023, **35**, 2207380.
30. T. Ikuno, J. Zheng, A. Vjunov, M. Sanchez-Sanchez, M. A. Ortuño, D. R. Pahls, J. L. Fulton, D. M. Camaioni, Z. Li, D. Ray, B. L. Mehdi, N. D. Browning, O. K. Farha, J. T. Hupp, C. J. Cramer, L. Gagliardi and J. A. Lercher, *J. Am. Chem. Soc.*, 2017, **139**, 10294-10301.
31. C.-W. Kung, J. E. Mondloch, T. C. Wang, W. Bury, W. Hoffeditz, B. M. Klahr, R. C. Klet, M. J. Pellin, O. K. Farha and J. T. Hupp, *ACS Appl. Mater. Interfaces*, 2015, **7**, 28223-28230.
32. Z. Li, A. W. Peters, J. Liu, X. Zhang, N. M. Schweitzer, J. T. Hupp and O. K. Farha, *Inorg. Chem. Front.*, 2017, **4**, 820-824.
33. D. Yang, S. O. Odoh, J. Borycz, T. C. Wang, O. K. Farha, J. T. Hupp, C. J. Cramer, L. Gagliardi and B. C. Gates, *ACS Cat.*, 2016, **6**, 235-247.
34. J. Zheng, J. Ye, M. A. Ortuño, J. L. Fulton, O. Y. Gutiérrez, D. M. Camaioni, R. K. Motkuri, Z. Li, T. E. Webber, B. L. Mehdi, N. D. Browning, R. L. Penn, O. K. Farha, J. T. Hupp, D. G. Truhlar, C. J. Cramer and J. A. Lercher, *J. Am. Chem. Soc.*, 2019, **141**, 9292-9304.
35. H. Liu, M. Cheng, Y. Liu, J. Wang, G. Zhang, L. Li, L. Du, G. Wang, S. Yang and X. Wang, *Energy & Environmental Science*, 2022, **15**, 3722-3749.
36. G. Durin, M. Y. Lee, M. A. Pogany, T. Weyhermuller, N. Kaeffer and W. Leitner, *J. Am. Chem. Soc.*, 2023, **145**, 17103-17111.
37. S. Gnaim, A. Bauer, H. J. Zhang, L. Chen, C. Gannett, C. A. Malapit, D. E. Hill, D. Vogt, T. Tang, R. A. Daley, W. Hao, R. Zeng, M. Quertenmont, W. D. Beck, E. Kandahari, J. C. Vantourout, P. G. Echeverria, H. D. Abruna, D. G. Blackmond, S. D. Minteer, S. E. Reisman, M. S. Sigman and P. S. Baran, *Nature*, 2022, **605**, 687-695.
38. K. C. Cartwright, A. M. Davies and J. A. Tunge, *Eur. J. Org. Chem.*, 2020, **2020**, 1245-1258.
39. D. Dolui, S. Khandelwal, P. Majumder and A. Dutta, *Chem. Commun.*, 2020, **56**, 8166-8181.
40. S. Roy, Z. Huang, A. Bhunia, A. Castner, A. K. Gupta, X. Zou and S. Ott, *J Am Chem Soc*, 2019, **141**, 15942-15950.
41. J. L. Dempsey, B. S. Brunschwig, J. R. Winkler and H. B. Gray, *Acc. Chem. Res.*, 2009, **42**, 1995-2004.
42. A. Suzuki, Y. Kamei, M. Yamashita, Y. Seino, Y. Yamaguchi, T. Yoshino, M. Kojima and S. Matsunaga, *Angew. Chem. Int. Ed.*, 2023, **62**, e202214433.
43. Y. Kamei, Y. Seino, Y. Yamaguchi, T. Yoshino, S. Maeda, M. Kojima and S. Matsunaga, *Nat. Commun.*, 2021, **12**, 966.
44. M. Kojima and S. Matsunaga, *Trends Chem.*, 2020, **2**, 410-426.
45. S. Jana, V. J. Mayerhofer and C. J. Teskey, *Angew. Chem. Int. Ed.*, 2023, **62**, e202304882.
46. T. Lazarides, T. McCormick, P. Du, G. Luo, B. Lindley and R. Eisenberg, *J Am Chem Soc*, 2009, **131**, 9192-9194.
47. M. Ming, H. Yuan, S. Yang, Z. Wei, Q. Lei, J. Lei and Z. Han, *J. Am. Chem. Soc.*, 2022, **144**, 19680-19684.

48. Z. Guo, G. Chen, C. Cometto, B. Ma, H. Zhao, T. Groizard, L. Chen, H. Fan, W.-L. Man, S.-M. Yiu, K.-C. Lau, T.-C. Lau and M. Robert, *Nat. Catal.*, 2019, **2**, 801-808.
49. Z. Guo, S. Cheng, C. Cometto, E. Anxolabéhère-Mallart, S.-M. Ng, C.-C. Ko, G. Liu, L. Chen, M. Robert and T.-C. Lau, *J. Am. Chem. Soc.*, 2016, **138**, 9413-9416.
50. H. Rao, L. C. Schmidt, J. Bonin and M. Robert, *Nature*, 2017, **548**, 74-77.
51. J. Bu, Z. Liu, W. Ma, L. Zhang, T. Wang, H. Zhang, Q. Zhang, X. Feng and J. Zhang, *Nat. Catal.*, 2021, **4**, 557-564.
52. L. Buglioni, F. Raymenants, A. Slattery, S. D. A. Zondag and T. Noel, *Chem. Rev.*, 2022, **122**, 2752-2906.
53. E. Zhao, W. Zhang, L. Dong, R. Zbořil and Z. Chen, *ACS Catal.*, 2023, **13**, 7557-7567.
54. P. Du, J. Schneider, G. Luo, W. W. Brennessel and R. Eisenberg, *Inorg. Chem.*, 2009, **48**, 4952-4962.
55. N. E. Tokel-Takvoryan, R. E. Hemingway and A. J. Bard, *J. Am. Chem. Soc.*, 1973, **95**, 6582-6589.
56. X. Hu, B. S. Brunschwig and J. C. Peters, *J. Am. Chem. Soc.*, 2007, **129**, 8988-8998.
57. B. de Bruin, W. I. Dzik, S. Li and B. B. Wayland, *Chem. Eur. J.*, 2009, **15**, 4312-4320.
58. X.-J. Qi, Z. Li, Y. Fu, Q.-X. Guo and L. Liu, *Organometallics*, 2008, **27**, 2688-2698.
59. Y. Xiao, C.-M. Zhu, R.-B. Liang, Y.-L. Huang, C.-H. Hai, J.-R. Chen, M. Li, J.-J. Zhong and X.-C. Huang, *Chem. Commun.*, 2023, **59**, 2239-2242.
60. H. Dai, R. Zhang, Z. Liu, W. Jiang and Y. Zhou, *Chem. Eur. J.*, 2024, **30**, e202302816.
61. W. Zhang, R. Huang, L. Song and X. Shi, *Nanoscale*, 2021, **13**, 9075-9090.
62. P. M. Stanley, A. Y. Su, V. Ramm, P. Fink, C. Kimna, O. Lieleg, M. Elsner, J. A. Lercher, B. Rieger, J. Warnan and R. A. Fischer, *Adv. Mater.*, 2023, **35**, e2207380.